CHEMISTRY
A EUROPEAN JOURNAL

G–G Base-Pairing in Nucleobase Adducts of the Anticancer Drug *cis*-[$PtCl_2(NH_3)$(2-picoline)] and Its *trans* Isomer

Geraldine McGowan, Simon Parsons, and Peter J. Sadler*[a]

Abstract: *cis*-[$PtCl_2(NH_3)$(2-picoline)] (AMD473) is a sterically-hindered anticancer complex with a profile of chemical and biological activity that differs significantly from that of cisplatin. Adducts of AMD473 with neutral 9-ethylguanine (9-EtGH) and anionic (N1-deprotonated) 9-ethylguanine (9-EtG) as perchlorate and nitrate salts, and also a nitrate salt of the *trans* isomer (AMD443), were prepared and their structures determined by X-ray crystallography: *cis*-[$Pt(NH_3)$(2-pic)(9-EtGH)$_2$]$(ClO_4)_2$ (**1**)·2H_2O·Me_2CO, *cis*-[$Pt(NH_3)$(2-pic)(9-EtGH)$_2$]$(NO_3)_2$ (**2**)·2H_2O, *cis*-[$Pt(NH_3)$(2-pic)(9-EtGH)(9-EtG)]NO_3 (**3**)·3.5H_2O, *trans*-[$Pt(NH_3)$(2-pic)(9-EtGH)(9-EtG)]NO_3 (**4**)·8H_2O. In all cases, platinum coordination is through N7 of neutral (**1**, **2**) and anionic (**3**, **4**) guanine. In each complex, the guanine bases are arranged in the head-to-tail conformation. In complex **1**, there is an infinite array of six-molecule cycles, based on both hydrogen bonding and π–π stacking of the 2-picoline and guanine rings.

Keywords: anticancer drug · guanine · hydrogen bonding · platinum · X-ray crystallography

Platinum(II) coordinated at N7 acidifies the N1 proton of neutral 9-ethylguanine ($pK_a = 9.57$) to give $pK_{a1} = 8.40$ and $pK_{a2} = 8.75$ for complex **2**, and $pK_{a1} = 7.77$ and $pK_{a2} = 9.00$ for complex **4**. In complexes **3** and **4**, three intermolecular hydrogen bonds are formed between neutral and deprotonated guanine ligands involving O6, N1 and N2 sites. Unusually, both of the platinated guanine bases of complexes **3** and **4** participate in this triple G≡G hydrogen bonding. This is the first report of X-ray crystal structures of nucleobase adducts of the promising anticancer drug AMD473.

Introduction

Cisplatin, the world's best-selling anticancer drug, has been the subject of intense research over the last 35 years. The antitumour activity of cisplatin and various other anticancer platinum drugs is attributed to their ability to modify the structure of the DNA of cancer cells.[1] Cisplatin reacts with genomic DNA and yields a variety of monoadducts and intra- and interstrand cross-links,[2] as well as protein–DNA cross-links.[1]

The most nucleophilic sites in duplex DNA are guanine (G) residues, especially those located adjacent to a second guanine residue. For Pt^{II} coordination, guanine N7 appears to be the preferred binding site. Therefore, it is not surprising that the major adduct of cisplatin with DNA is an intrastrand cross-link between the N7 atoms of adjacent guanine residues.[3] The coordinated guanine bases are orientated in a head-to-head (HH) conformation. However, the head-to-tail (HT) forms, characteristic of minor interstrand adducts, are thermodynamically favoured in all simple *cis*-[PtA_2G_2] models (A = amine or half of a diamine), and the head-to-head form is relatively rare.[3,4]

cis-[$PtCl_2(NH_3)$(2-picoline)] (AMD473) is a sterically hindered anticancer complex with a profile of chemical and biological activity that differs significantly from that of cisplatin.[5] AMD473 has been administered to over 500 cancer patients in phase I and phase II clinical trials, in which it has demonstrated activity against a wide range of tumours and a manageable safety profile. AMD473 also has the potential to be administered as an oral formulation. The 2-methyl group hinders axial approach to Pt^{II} in AMD473, and as a result, hydrolysis occurs approximately four times more slowly than for cisplatin.[6] The introduction of steric bulk by the 2-picoline ligand (Figure 1) in AMD473, may give rise to novel DNA platination reactions, such as differential binding to nucleobases and structures locked in a single conformation. To gain further insight into stereochemical effects on the structure and dynamics of nucleobase adducts, we

[a] G. McGowan, Dr. S. Parsons, Prof. P. J. Sadler
School of Chemistry, The University of Edinburgh
King's Buildings, West Mains Road, Edinburgh EH9 3JJ (UK)
Fax: (+44) 131-650-6453
E-mail: p.j.sadler@ed.ac.uk

Supporting information for this article is available on the WWW under http://www.chemeurj.org/ or from the author.

DOI: 10.1002/chem.200500122

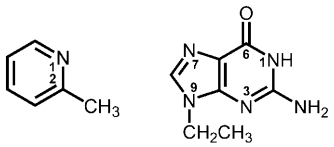

Figure 1. Schematic representation of 2-picoline (left) and 9-ethylguanine (9-EtGH, right), including conventional numbering.

studied adducts of AMD473 and its *trans* isomer, *trans*-$[PtCl_2(NH_3)(2\text{-pic})]$ (AMD443), with 9-ethylguanine (9-EtGH) (Figure 1) in solution and in the solid state. The *trans* isomer also exhibits high cytotoxicity in a variety of cancer cell-lines.[7]

Results

X-ray crystallography: Crystals containing *cis*-$[Pt(NH_3)(2\text{-pic})(9\text{-EtGH})_2]X_2$ ($X = ClO_4$, **1**·$2H_2O$·Me_2CO; $X = NO_3$, **2**·$2H_2O$) and *cis*-(**3**·$3.5H_2O$) or *trans*-(**4**·$8H_2O$) $[Pt(NH_3)(2\text{-pic})(9\text{-EtGH})(9\text{-EtG})]NO_3$ were obtained by reaction of the respective isomer of $[PtCl_2(NH_3)(2\text{-pic})]$ with slightly less than 2 mol equivalents of Ag^+, followed by reaction with 2 mol equivalents of 9-ethylguanine in water, and recrystallisation from acetone in the case of complex **1**, from water at pH 3.55 for complex **2**, and from water at pH 7.98 and 7.83 for complexes **3** and **4**, respectively. Crystallographic data and details of the refinement are listed in Table 1. Selected bond lengths and angles are given in Table 2, and the cations of **1**–**4** are shown in Figure 2. Hydrogen bond lengths and angles are given in Table 3. Rocking angles (Δ) and torsion angles (β) are listed in the Supporting Information.

Table 2. Selected bond lengths [Å] and angles [°] for **1**–**4**, in which **1** = *cis*-$[Pt(NH_3)(2\text{-pic})(9\text{-EtGH})_2](ClO_4)_2$, **2** = *cis*-$[Pt(NH_3)(2\text{-pic})(9\text{-EtGH})_2](NO_3)_2$, **3** = *cis*-$[Pt(NH_3)(2\text{-pic})(9\text{-EtGH})(9\text{-EtG})]NO_3$ and **4** = *trans*-$[Pt(NH_3)(2\text{-pic})(9\text{-EtGH})(9\text{-EtG})]NO_3$.

Bond/Angle[a]	**1**	**2**	**3**	**4**[b]
Pt–N(1)	2.041(5)	2.023(4)	2.047(4)	2.034(7)
Pt–N(13)	2.018(5)	2.019(4)	2.022(4)	2.047(8)
Pt–N(71)	2.008(4)	2.015(4)	2.009(4)	1.999(6)
Pt–N(72)	2.018(5)	2.020(4)	2.017(4)	2.011(6)
N(13)-Pt-N(1)	90.99(19)	88.18(15)	90.03(16)	177.8(3)
N(72)-Pt-N(1)	179.05(15)	178.74(17)	178.53(15)	90.0(3)
N(71)-Pt-N(1)	90.11(18)	88.31(15)	89.26(16)	89.1(3)
N(72)-Pt-N(13)	89.37(18)	91.69(15)	89.94(15)	91.2(3)
N(71)-Pt-N(13)	175.18(16)	174.70(14)	177.53(14)	89.8(3)
N(71)-Pt-N(72)	89.60(17)	91.90(14)	90.83(15)	178.5(3)
PtN_4/G1	73.62(19)	72.22(14)	86.00(15)	71.0(3)
PtN_4/G2	71.24(19)	52.83(19)	70.78(17)	58.0(3)
G1/G2	86.17(18)	71.25(14)	88.39(15)	51.9(3)

[a] The crystallographic atomic numbering schemes (Figure 2) differ from the chemical numbering scheme used in the text. [b] The numbering scheme in complex **4** differs from that of the *cis* complexes, but for comparison, N11 = N71 and N12 = N72.

In each complex, platinum coordination is through the N(7) sites of the two 9-ethylguanine ligands, which adopt the head-to-tail orientation. Platinum(II) has the usual square-planar geometry, and Pt–N bond lengths range from 1.999(6) to 2.047(8) Å, which is within the normal range for these types of complexes.

In complex **1**·$2H_2O$·Me_2CO, *cis*-$[Pt(NH_3)(2\text{-pic})(9\text{-EtGH})_2](ClO_4)_2$·$2H_2O$·$Me_2CO$, the *cis* 9-ethylguanine ligands are approximately perpendicular to one another (Figure 2a). The large dihedral angle of 86.17(18)° between the guanine bases prevents any substantial intramolecular base–base interaction. The plane angles of the 9-ethylguanine ligands relative to the 2-picoline are 89.2(3) and 6.0(3)°. There is high thermal motion and at temperatures lower than 240 K, the system appeared to undergo a phase change, but no data were collected at lower temperatures. The ethyl groups at the 9-position are disordered. There is intermolecular π–π stacking between 2-picoline and guanine rings (interplanar spacing 3.85–4.24 Å). In addition, there are hydrogen bonds between NH_3 groups and the O6 of guanine

Table 1. Crystallographic data for complexes **1**–**4**, in which **1**·$2H_2O$·Me_2CO = *cis*-$[Pt(NH_3)(2\text{-pic})(9\text{-EtGH})_2](ClO_4)_2$·$2H_2O$·$Me_2CO$, **2**·$2H_2O$ = *cis*-$[Pt(NH_3)(2\text{-pic})(9\text{-EtGH})_2](NO_3)_2$·$2H_2O$, **3**·$3.5H_2O$ = *cis*-$[Pt(NH_3)(2\text{-pic})(9\text{-EtGH})(9\text{-EtG})]NO_3$·$3.5H_2O$ and **4**·$8H_2O$ = *trans*-$[Pt(NH_3)(2\text{-pic})(9\text{-EtGH})(9\text{-EtG})]NO_3$·$8H_2O$.

	1·$2H_2O$·Me_2CO	**2**·$2H_2O$	**3**·$3.5H_2O$	**4**·$8H_2O$
formula	$C_{23}H_{38}Cl_2N_{12}O_{13}Pt$	$C_{20}H_{32}N_{14}O_{10}Pt$	$C_{20}H_{34}N_{13}O_{8.5}Pt$	$C_{20}H_{43}N_{13}O_{13}Pt$
M_r	956.94	823.69	787.69	868.76
crystal system	triclinic	triclinic	triclinic	monoclinic
space group	$P\bar{1}$	$P\bar{1}$	$P\bar{1}$	$P2_1/n$
a [Å]	13.147(15)	11.9052(5)	8.8183(3)	16.0748(5)
b [Å]	14.056(16)	12.2098(4)	11.2332(4)	22.8397(8)
c [Å]	14.634(16)	12.4032(4)	15.7824(5)	17.5291(6)
α [°]	87.783(17)	72.813(2)	95.894(2)	90
β [°]	84.728(17)	65.613(2)	97.663(2)	97.891(2)
γ [°]	66.668(15)	67.423(2)	112.685(2)	90
V [Å^3]	2473(5)	1495.98(9)	1409.09(8)	6374.8(4)
Z	2	2	2	8
λ [Å]	0.71073	0.71073	0.71073	0.71073
T [K]	240(2)	150(2)	293(2)	150(2)
ρ_{calcd} [g cm^{-3}]	1.285	1.829	1.857	1.810
μ_{calcd} [mm^{-1}]	3.001	4.766	5.050	4.486
$F(000)$	952	816	782	3488
2θ range [°]	1.80–28.92	1.83–28.88	1.32–28.99	1.47–25.00
reflns. collected	20627	27532	13990	38056
independent reflns.	11352	12830	6655	11215
reflns.(R_{int})	(0.0469)	(0.0489)	(0.0258)	(0.0654)
$R1$ [$F_0 > 4\sigma(F_0)$]	0.0477	0.0373	0.0353	0.0586
$wR2$ (all data)	0.1114	0.0929	0.0847	0.1424

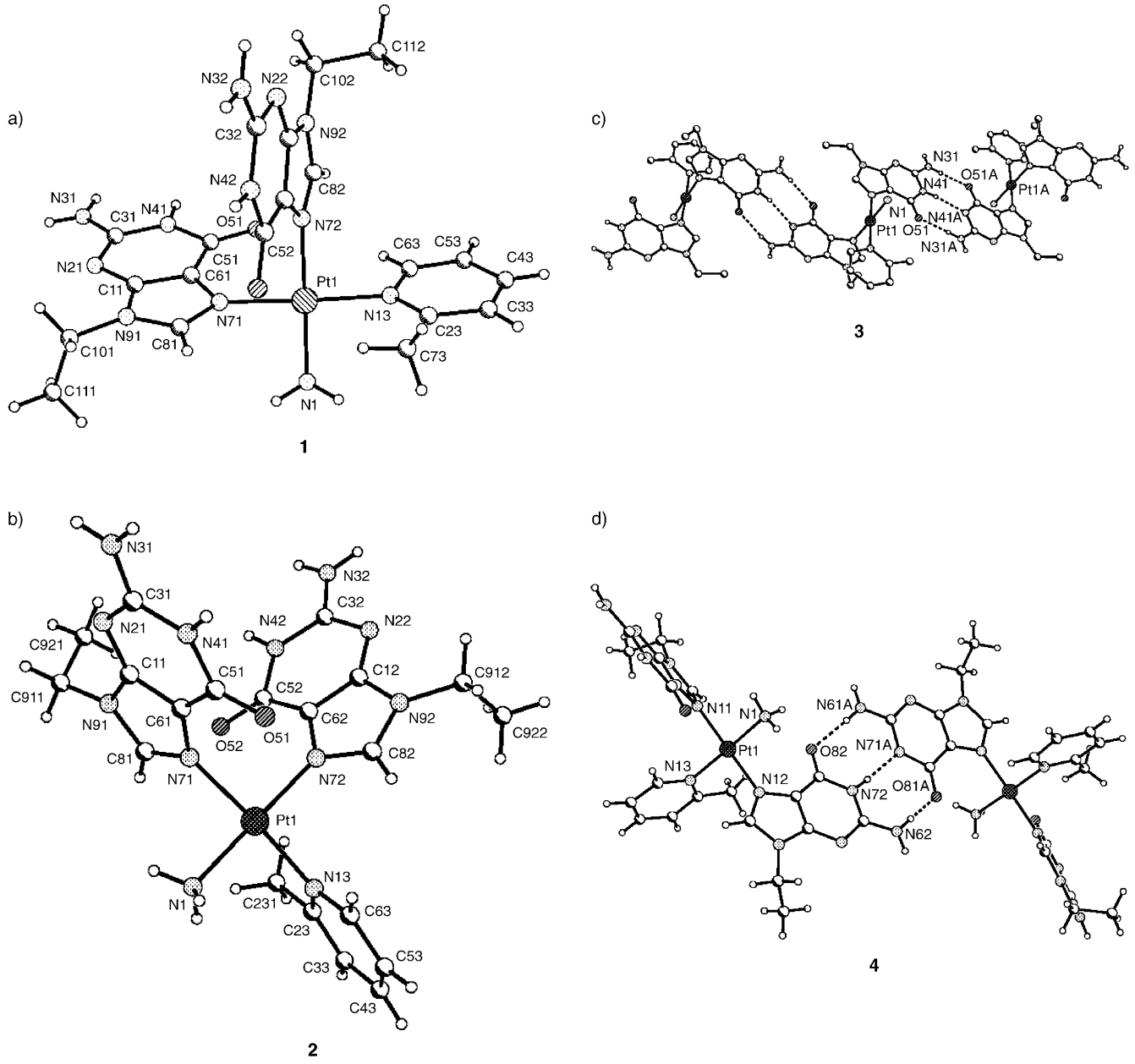

Figure 2. a) The cation *cis*-$[Pt(NH_3)(2\text{-pic})(9\text{-EtGH})_2]^{2+}$ in complex **1**. The planes of the 9-EtGH and 2-picoline rings are 70–80° relative to the Pt square-plane. The 9-EtGH bases are approximately perpendicular to one another. Intermolecular interactions are shown in Figure 3. b) The cation *cis*-$[Pt(NH_3)(2\text{-pic})(9\text{-EtGH})_2]^{2+}$ in complex **2**. The change in the anion compared to complex **1** has resulted in a significant decrease in the angle between the guanine base *cis* to 2-picoline and the Pt square-plane. The dihedral angle between the guanine bases is also reduced. There are additional hydrogen-bond interactions mediated by the anion. c) Intermolecular triple hydrogen bonding in the structure of complex **3**, *cis*-$[Pt(NH_3)(2\text{-pic})(9\text{-EtGH})(9\text{-EtG})]^{+}$. The guanine bases are almost perpendicular to one another and each of the guanine bases and the 2-picoline are tilted by 70–80° relative to the platinum square-plane. The cations form an infinite chain with π–π stacking. d) Intermolecular triple hydrogen bonding in the structure of complex **4**, *trans*-$[Pt(NH_3)(2\text{-pic})(9\text{-EtGH})(9\text{-EtG})]^{+}$. Two molecules are shown, which form part of an infinite chain. The dihedral angle between the guanine bases is much smaller in this case, only 52°. The crystallographic numbering relates to the chemical numbering given in Figure 1, as follows: Complexes **1** and **2**: N71, N72 = N7. Complex **3**: N31 = $C2NH_2$; N41 = N1; O51 = O6. Complex **4**: N11, N12 = N7; O82 = O6; N71, N72 = N1; N61, N62 = $C2NH_2$.

(N−O = 2.88 Å), as well as double hydrogen bonds between N3 positions and NH_2 groups (N−N = 3.00, 3.03 Å) on neighbouring molecules. These features combine to create an infinite array of six-molecule cycles (Figure 3).

In complex **2**·2 H_2O, *cis*-$[Pt(NH_3)(2\text{-pic})(9\text{-EtGH})_2](NO_3)_2$·2 H_2O, the dihedral angle between the *cis* 9-ethylguanine ligands is slightly smaller, 71.25(14)° (Figure 2b). The plane angles of the 9-ethylguanine ligands relative to 2-picoline are 76.5(2) and 20.4(2)°. There is extensive hydrogen bonding between NH_3, N1, $C2NH_2$ and the NO_3 counterion, and O6, N3 and $C2NH_2$ are involved in hydrogen bonding with solvent water molecules. The only intermolecular hy-

Table 3. Selected hydrogen bond lengths [Å] (with H···A < r(A)+2.000), and angles [°] (⩾DHA > 110).

D–H	d(D–H)	d(H···A)	⩾DHA	d(D···A)	A
1					
N1–H1C	0.900	2.090	146.40	2.883	O51[a]
N31–H31A	0.870	2.157	175.94	3.025	N21[b]
N32–H32A	0.870	2.137	169.77	2.997	N22[c]
2					
N32–H32A	0.880	2.055	166.61	2.919	O51[a]
3					
N31–H31B	0.860	1.971	178.08	2.831	O51[d]
N41–H41	0.860	2.078	172.81	2.934	N41[d]
N32–H32B	0.860	1.999	168.37	2.847	O52[c]
N42–H42	0.860	2.104	168.46	2.951	N42[c]
4					
N61–H61B	0.880	1.929	172.10	2.803	O82[e]
N62–H62B	0.880	2.084	166.03	2.945	O81[f]
N72–H72	0.880	2.059	177.00	2.938	N71[f]
N64–H64B	0.880	1.965	170.69	2.837	O85[e]
N74–H74	0.880	2.042	172.71	2.917	N75[e]
N65–H65A	0.880	1.964	164.04	2.821	O84[f]

Equivalent positions: [a] $-x$, $-y+1$, $-z+1$; [b] $-x$, $-y+2$, $-z+1$; [c] $-x+1$, $-y+1$, $-z$; [d] $-x+1$, $-y$, $-z+1$; [e] $x-1/2$, $-y+1/2$, $z-1/2$; [f] $x+1/2$, $-y+1/2$, $z+1/2$. Relationship between crystallographic and chemical numbering schemes: Complex **1**: N1 = NH_3; N31, N32 = $C2NH_2$; N21, N22 = N3; O51 = O6. Complex **2**: N32 = $C2NH_2$; O51 = O6. Complex **3**: N31, N32 = $C2NH_2$; N41, N42 = N1; O51, O52 = O6. Complex **4**: N61, N62, N64, N65 = $C2NH_2$; N71, N72, N74, N75 = N1; O81, O82, O84, O85 = O6.

drogen bonding is between the $C2NH_2$ group and O6 (N–O = 2.92 Å). There is also a weak stacking interaction between the guanine planes.

In the cation of complex **3**·3.5 H_2O, *cis*-[Pt(NH_3)(2-pic)(9-EtGH)(9-EtG)]NO_3·3.5 H_2O, the 9-ethylguanine ligands are again almost perpendicular to one another, with a dihedral angle of 88.39(15)° (Figure 2c). The plane angles of the 9-ethylguanine ligands relative to 2-picoline are 88.9(2) and 2.9(2)°. There is disorder about the Pt–N (pic) bond of 180° to give a distribution for the C2 and C6 positions of the 2-picoline ligand of 75 and 25%, respectively. There is intermolecular triple hydrogen bonding between the N1 of 9-EtG of one molecule and the N1H of 9-EtGH of an adjacent molecule (N–N = 2.93 Å), which, together with $C2NH_2$–O6 hydrogen bonds (N–O = 2.83 Å), gives rise to a G–G^- base pair. The proton shared between the two N1 atoms of the 9-ethylguanine ligands appears to be disordered over two positions, a 1:1 mixture of N1H–N1A and N1–HN1A.

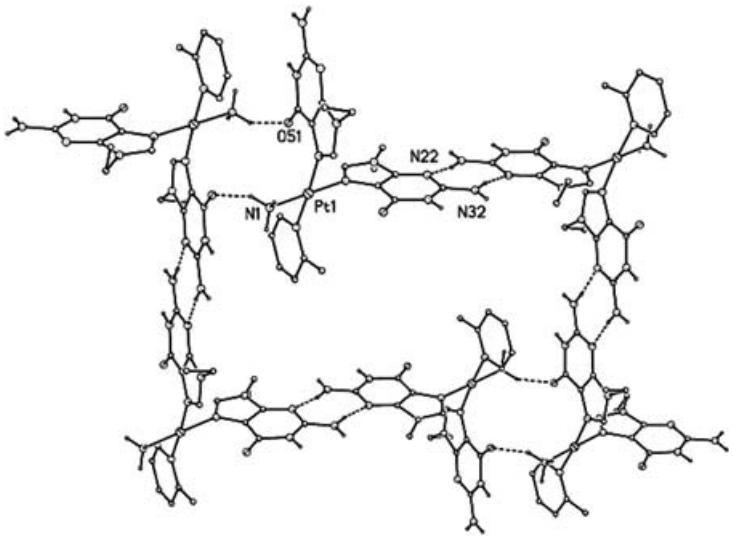

Figure 3. The six-molecule cyclic arrangement present in crystals of complex **1**. The intermolecular interactions involve alternating Pt–NH_3···O(6) hydrogen bonding, π–π 2-pic/9-EtGH stacking, and double N(2)H_2···N3, N3···H_2N(2) hydrogen bonding.

The *trans* 9-ethylguanine ligands in the cation of complex **4**·8 H_2O, *trans*-[Pt(NH_3)(2-pic)(9-EtGH)(9-EtG)]NO_3·8 H_2O, have a dihedral angle of 51.9(3)°, and the plane angles of the 9-ethylguanine ligands relative to the 2-picoline ligand are 85.5(5) and 81.2(5)° (Figure 2d). This complex forms a triple hydrogen bond, similar to that in complex **3**, giving rise to a G–G^- base pair. The hydrogen bond lengths are 2.80–2.95 Å for NH_2–O6 and 2.92–2.94 Å for N1(H)–N1. There are effectively two parallel chains formed through π–π stacking, which run in the same direction and interact with one another.

Solution studies

cis-*[Pt(NH$_3$)(2-pic)(9-EtGH)$_2$](ClO$_4$)$_2$* (***1***): The peak at m/z = 763 in the positive-ion electrospray mass spectrum of complex **1** in water was assigned to the parent ion with an associated ClO_4^- counterion, $[Pt(NH_3)(2\text{-pic})(9\text{-EtGH})_2\cdot ClO_4]^+$. The other peaks were assigned as follows: m/z 584 $[Pt(NH_3)(2\text{-pic})(9\text{-EtGH})\cdot ClO_4]^+$, m/z 483 $[Pt(NH_3)(2\text{-pic})(9\text{-EtGH})-H]^+$, m/z 466 $[Pt(2\text{-pic})(9\text{-EtGH})-H]^+$.

The ^{1}H NMR spectra of complex **1** in D_2O and acetone at 298 K are shown in Figure S1 (see Supporting Information). Clearly, the solvent has a large effect on chemical shift; however, most noticeable is that the H8 signals for the 9-ethylguanine ligands are indistinguishable in aqueous solution, whereas in acetone, they are separated by 0.2 ppm. Therefore, we examined the change in chemical shift of H8 in various acetone/H_2O mixtures. The spectra (Figure S2, Supporting Information) show the convergence of the two H8 signals as the molar fraction of water increases. The variation in chemical shift is plotted in Figure 4a. The chemical shift of one of the H8 peaks (G1H8) is solvent dependent to a much greater extent than the other (G2H8).

The temperature dependence of the ^{1}H NMR spectrum of complex **1** in D_2O was further investigated between 278 and 313 K (Figure S3, Supporting Information). At low temperature, there are two individual H8 signals. Although the resonance for the H8 proton of one of the 9-ethylguanine ligands (G1H8) appears to be highly temperature dependent, the H8 peak for the other 9-ethylguanine (G2H8) is almost unaffected. This is clearly demonstrated by the plot of δ H8 shift versus temperature, shown in Figure 4b.

A two-dimensional ROESY spectrum of complex **1** in acetone (Figure 5) was recorded at 278 K to investigate the solution structure of this complex. Only one of the two H8

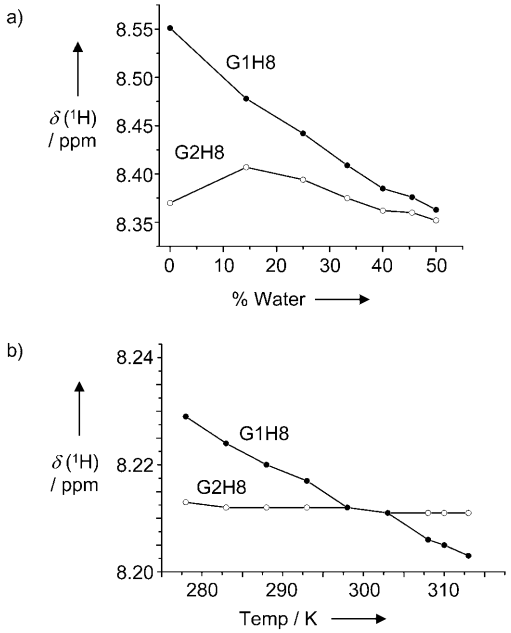

Figure 4. a) Plot of δ H8 for the two 9-EtGH ligands in complex **1** in [D_6]acetone versus the % (v/v) of water, showing how the separation of the H8 signals decreases as the percentage of water increases. b) Plot of δ H8 versus temperature for complex **1** in D_2O.

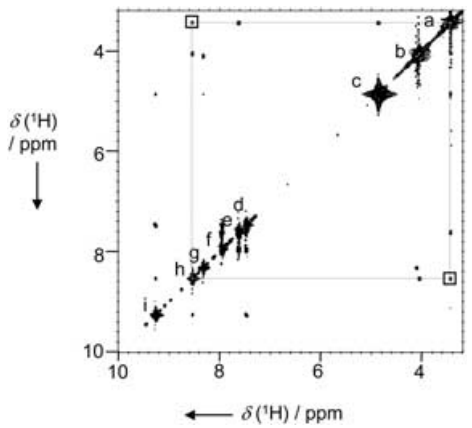

Figure 5. Two-dimensional [^{1}H,^{1}H] ROESY NMR spectrum of complex **1** in [D_6]acetone at 278 K. Assignments: a = 2-pic CH_3; b = Et CH_2; c = NH_3; d = H5 2-pic; e = H3 2-pic; f = H4 2-pic; g = H8 of 9-EtGH (G2); h = H8 of 9-EtGH (G1); i = H6 2-pic.

signals (G1H8) exhibits an NOE cross-peak to the 2-picoline methyl group. This H8 signal (G1H8) also exhibits an NOE cross-peak to the aromatic H6 proton of the 2-picoline ligand.

trans-*[Pt(NH$_3$)(2-pic)(9-EtGH)(9-EtG)]NO$_3$·8H$_2$O* (***4***): Positive-ion electrospray mass spectrometry showed peaks for the parent ion at $m/z = 662$, assigned to $[Pt(NH_3)(2\text{-pic})(9\text{-EtGH})_2\text{-H}]^+$, together with peaks assignable to fragments: $m/z = 645$ $[Pt(2\text{-pic})(9\text{-EtGH})_2\text{-H}]^+$, $m/z = 466$ $[Pt(2\text{-pic})(9\text{-EtGH})\text{-H}]^+$.

The ^{1}H NMR spectrum of complex **4**, recorded in H_2O/D_2O 9:1 (Figure S4, Supporting Information), contains only one set of peaks, corresponding to the two coordinated 9-ethylguanine ligands. The ^{1}H NMR chemical shifts of the peaks of complex **4** were not temperature dependent between 278 and 318 K. A two-dimensional NOESY spectrum revealed that there is an NOE cross-peak for the H8 signal of the 9-ethylguanine ligands and the 2-picoline CH_3 group.

In the pH range from 2–12, the pH-dependent ^{1}H NMR chemical shift measurements for complex **2** in H_2O/D_2O 9:1 show two acid–base equilibria, corresponding to the deprotonation of the two inequivalent N1H sites of the 9-ethylguanine ligands (Figure 6a). The pK_a values are 8.40 and

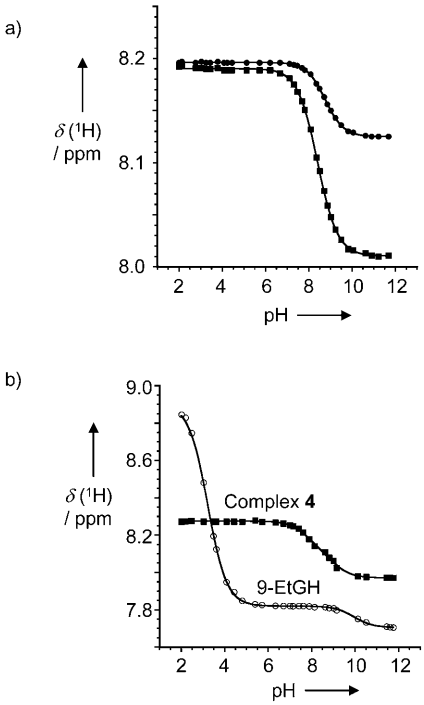

Figure 6. Dependence of the H8 chemical shifts of a) complex **2** and b) complex **4** and free 9-ethylguanine on pH. Note that there are two distinguishable H8 peaks for complex **2**, but unambiguous assignments cannot be made. The solution of **4** also contained a small amount of free 9-ethylguanine. The curves are computer fits to the Henderson–Hasselbalch equation, and give the pK_a values listed in Table 4.

8.75. Complex **4** also has two acid–base equilibria (Figure 6b), with pK_a values of 7.77 and 9.00. The pK_a values for free 9-ethylguanine under the same conditions were determined to be 3.22 (N7) and 9.94 (N1H).

Discussion

In the past, structural investigations of platinum–nucleobase complexes concentrated almost exclusively on cisplatin compounds,[8–23] and consequently, relatively few structural studies of nucleobase complexes of *trans* Pt^{II} compounds have

been reported. Details of many of these *trans* complexes are summarised in a review by Lippert.[24] Here, we studied bis-nucleobase adducts of the sterically-hindered anticancer compound *cis*-$[PtCl_2(NH_3)(2\text{-pic})]$ (AMD473) and its *trans* isomer AMD443. Three crystal structures of AMD473 adducts and one of an AMD443 adduct containing the model nucleobase 9-ethylguanine were determined (**1**–**4**). These are the first X-ray structures of nucleobase adducts of $[PtCl_2(NH_3)(2\text{-pic})]$ anticancer complexes.

Coordination at the N7 position of guanine was confirmed in each case, as was a head-to-tail orientation of the bases. The head-to-tail forms are characteristic of the minor interstrand adducts formed by cisplatin with DNA, and are thermodynamically favoured in all simple *cis*-$[PtA_2G_2]$ models (A = amine or half of a diamine, G = guanine derivative).[3] However, there are few examples of the head-to-head conformation, which is the more realistic model for a Pt–DNA complex.[8–10]

The main difference between complexes **1** and **2** is the anion; perchlorate and nitrate, respectively. Complex **1** exhibits a rare case of negative rocking angles (−7.68, −5.25°; i.e., C(8)-N(7)-Pt angles > C(5)-N(7)-Pt angles). For complex **2**, the rocking angles are positive, as observed typically in structures of related complexes.[25] In complex **2**, the nitrate anion acts as a spacer between molecules and dominates the hydrogen-bond interactions. Consequently, there is only one type of intermolecular hydrogen bond, between $C2NH_2$ and O6, and hence complex **2** is unable to form the type of cycle described for **1**. Other structural differences may be simply a consequence of crystal packing. Complexes **2** and **3** differ in the charge on the complex and in the number of counterions and water molecules in the unit cell. A further and most intriguing difference is that in complex **2**, the guanine base in the head orientation with respect to the methyl group of 2-picoline is *trans* to the 2-picoline ligand, whereas in complex **3**, the analogous guanine base is *cis* to the 2-picoline ligand. This indicates that both head-to-tail orientations of 9-ethylguanine relative to the *cis* 2-picoline ligand are possible, although intermolecular interactions may favour only one of these orientations. It is expected that complexes **1**, **2** and **3** adopt the same structure in solution (at the same pH).

Complex **4** is a rare example of a bisguanine–Pt^{II} complex that has a large dihedral angle of 51.9(3)° between the two purine bases. Another example is *trans*-$[Pt(MeNH_2)_2(1\text{-MeC})_2](PF_6)_2$, with a dihedral angle of 56(1)°.[26] In most other bis(nucleobase) complexes of *trans*-$[(am)_2Pt]$, the bases are reasonably coplanar.[26–30] This large dihedral angle may result from the steric hindrance imposed by the bulky 2-picoline ligand.

Complexes **3** and **4** have the most interesting structural features. Both exhibit intermolecular triple hydrogen bonding involving NH_2, NH and O6, which gives rise to a G–G^- base pair. There are various reports[20–23,26,27,31,32] of PtG^-–G and PtG^-–GPt hydrogen bonding caused by deprotonation at the N1 position of Pt^{II}-bound guanine. Five X-ray structures for such complexes have been reported. Three of these are monoguanine complexes: *cis*-$[Pt(NH_3)_2(9\text{-EtGH})(1\text{-MeC})][Pt(NH_3)_2(9\text{-EtG})(1\text{-MeC})](ClO_4)_3$,[21] *trans*-$[\{Pt(NH_3)_2(tmade)(9\text{-EtGH})\}\{Pt(NH_3)_2(tmade)(9\text{-EtG})\}](ClO_4)_2\cdot NO_3\cdot 1.6\,H_2O$ (in which tmade = $N^{6'},N^{6'},N^9$-trimethyladenine),[26] {*trans*, *trans*-$[(NH_3)_2Pt(1\text{-MeU})(9\text{-EtA})Pt(NH_2CH_3)_2(9\text{-EtGH}_{0.5})](ClO_4)_{2.5}\cdot 1.25\,H_2O\}_2$.[31] The other two, *cis*-$[Pt(NH_3)_2(9\text{-EtG})_2]\cdot 9\text{-EtGH}\cdot 7\,H_2O$[20] and $[\{Pt(NH_3)(9\text{-MeGH})_2(9\text{-MeG})\}\{Pt(NH_3)(9\text{-MeGH})_3\}\{1\text{-MeC}\}_4](ClO_4)_3\cdot 4\,H_2O$,[32] contain two coordinated guanine residues, but only one of these is involved in triple hydrogen bonding. In complexes **3** and **4**, both platinated guanine bases are involved in G≡G triple hydrogen bonding. As a result, complexes **3** and **4** form infinite chains, but complex **4** does so in a more zigzag manner. To the best of our knowledge, this is the first report of structures in which both platinated guanine bases participate in G≡G triple hydrogen bonding. The triple hydrogen bond lengths for complexes **3** and **4** range from 2.80–2.95 Å for NH_2···O6 and 2.92–2.95 Å for N1(H)···N1; these values are comparable with 2.83(1) and 2.90(1) Å, respectively, in *trans*-$[\{Pt(NH_3)_2(tmade)(9\text{-EtGH})\}\{Pt(NH_3)_2(tmade)(9\text{-EtG})\}]^{3+}$.[26]

For the cation in complex **1**, *cis*-$[Pt(NH_3)(2\text{-pic})(9\text{-EtGH})_2]^{2+}$, there are four different stereoisomers (2 × HT and 2 × HH). Because the 2-methyl group can be on the upper or lower side of the platinum plane, four geometrical head-to-tail isomers are possible. Only two of these will be distinguishable, however, by NMR spectroscopic analysis, and therefore, four H8 signals should be observed. In reality, only two H8 peaks are observed. An explanation for this is either fast interconversion of head-to-tail conformations on the NMR timescale, or the molecule is locked into a single configuration at this temperature. The two-dimensional ROESY spectrum of complex **1** at 278 K clearly shows an NOE cross-peak for only one of the two H8 signals of 9-ethylguanine (G1H8) and the methyl group of the 2-picoline ligand (Figure 5), suggesting a head-to-tail orientation of the guanine bases. If the solution structure was locked into the same configuration as that observed by X-ray crystallography for the solid state, the only observable NOE contact between the methyl group of the 2-picoline ligand and an H8 proton would correspond to the 9-ethylguanine ligand *trans* to 2-picoline. Interestingly, G1H8 exhibits a greater solvent and temperature dependence than the second H8 peak, G2H8 (Figure 4). It can be argued that the 9-ethylguanine *cis* to the 2-picoline exhibits the more marked temperature and solvent dependence, especially if there is rapid rotation about the Pt–N bonds. Rapid interconversion of head-to-tail conformers is common in Pt^{II}–diamine complexes.[33,34] Rapid rotation should give rise to H8···CH_3 NOEs for both coordinated guanine bases, whereas only one ROESY cross-peak is detected. This suggests that the two H8 peaks observed contain four overlapping H8 signals. The major contribution to the observed NOE is probably from the 9-ethylguanine ligand *cis* to 2-picoline, in view of its intensity (medium compared to strong for the H6/H5 of 2-pic), and for which the H8···CH_3 distance is much shorter (ca. 3 Å versus 4.9 Å for a *trans* 9-ethylguanine; $NOE \propto r^{-6}$). Howev-

er, it is difficult to interpret NOEs quantitatively in a dynamic system. Moreover, the NOE cross-peak between the G1H8 peak and the aromatic H6 peak of the 2-picoline ligand further substantiates the argument that G1H8 corresponds to the 9-ethylguanine ligand *cis* to 2-picoline.

For *trans*-$[Pt(NH_3)(2\text{-pic})(9\text{-EtGH})_2]^{2+}$ from **4**, there are also four different stereoisomers ($2\times$HT and $2\times$HH; Figure 7). The two HT isomers (Figure 7a) are enantiomers.

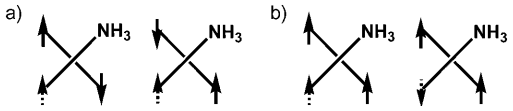

Figure 7. a) Head-to-tail enantiomers of *trans*-$[Pt(NH_3)(2\text{-pic})(9\text{-EtGH})_2]^{2+}$. b) Head-to-head isomers of *trans*-$[Pt(NH_3)(2\text{-pic})(9\text{-EtGH})_2]^{2+}$. Solid arrows represent the orientation of the 9-ethylguanine ligands, and dotted arrows represent that of the 2-picoline methyl group with respect to the platinum square-plane.

Therefore, only one HT configuration will be observed by NMR spectroscopic analysis. As the two 9-ethylguanine ligands are in slightly different environments, we expect to observe two sets of peaks, however, experimentally, only one set of peaks is observed. This could be due to fast rotation about the Pt–2-pic bond, or to fast rotation of the guanine bases. Although Reedijk and co-workers[35] reported slow rotation about the Pt–2-pic bonds at room temperature in *cis*-$[Pt(2\text{-pic})_2(Puo)_2]^{2+}$ (Puo = guanosine or 9-methylhypoxanthine), they confirmed that rotation of these 6-oxopurines from -30 to $+90\,^{\circ}C$ is fast on the NMR timescale.

The pK_a values of 8.40 and 8.75 for complex **2**, and 7.77 and 9.00 for complex **4**, which are assignable to N1H deprotonation of coordinated 9-ethylguanine, are 0.6–1.8 units lower than that for free 9-ethylguanine (Table 4). This observed acidification is a consequence of the inductive effect of Pt at the N7 position of guanine, and lies within the range observed for similar amine complexes (Table 4).

Table 4. Comparison of pK_a values for N1H of 9-EtGH in the complexes studied here (**2** and **4**), and for reported cisplatin adducts.

Species	pK_a N1(H)	Reference
9-ethylguanine	9.57	[36]
cis-$[Pt(NH_3)(2\text{-pic})(9\text{-EtGH})_2]^{2+}$	8.40, 8.75	present work
trans-$[Pt(NH_3)(2\text{-pic})(9\text{-EtGH})_2]^{2+}$	7.77, 9.00	present work
cis-$[Pt(NH_3)_2(9\text{-EtGH})_2]^{2+}$	7.76, 8.36	[36]
cis-$[Pt(NH_3)_2(9\text{-EtGH})_2]^{2+}$	8.01, 8.66	[37]
trans-$[Pt(NH_3)_2(9\text{-EtGH})_2]^{2+}$	7.90, 8.54	[37]

The guanine–guanine pairing pattern observed in complexes **3** and **4** represents a model for a nucleobase mispair. There is probably little chance of formation of such a guanine pair in DNA, as it is necessary to have independently metallated guanine bases in close proximity. However, with RNA and its enormous structural diversity, such possibilities are more likely.

Conclusion

In this study of bisnucleobase adducts of the sterically-hindered anticancer drug AMD473 and its *trans* isomer AMD443, we synthesised and characterised three AMD473 adducts and an AMD443 adduct containing 9-ethylguanine. Each of the complexes has a head-to-tail arrangement of the guanine bases in contrast to the head-to-head arrangement preferred in DNA. Platination at the N7 position was confirmed in each case. Interesting triple hydrogen bonding was revealed in the structures of both the *cis* and *trans* 9-ethylguanine adducts, giving rise to G–G$^-$ base pairs for both coordinated guanine bases. The pK_a value of N1H of 9-ethylguanine was lowered significantly by N7 coordination to Pt^{II}, most notably for the *trans* complex (**4**) relative to free 9-ethylguanine.

Experimental Section

Preparations: 9-Ethylguanine was purchased from Sigma. *cis*-$[PtCl_2(NH_3)(2\text{-pic})]$ was kindly provided by AstraZeneca. The synthesis of *trans*-$[PtCl_2(NH_3)(2\text{-pic})]$ was based on previously published procedures.[38]

cis-*[Pt(NH$_3$)(2-pic)(9-EtGH)$_2$](ClO$_4$)$_2$ (**1**)·2 H$_2$O·Me$_2$CO*: *cis*-$[PtCl_2(NH_3)(2\text{-pic})]$ was reacted with 1.98 equiv of $AgClO_4$ (5 h, 323 K), followed by filtration of AgCl, and then addition of 2 mol equiv of 9-EtGH (4 d, 323 K). Recrystallisation from acetone, and slow evaporation yielded **1** as colourless cubes.

cis-*[Pt(NH$_3$)(2-pic)(9-EtGH)$_2$](NO$_3$)$_2$ (**2**)·2 H$_2$O*: *cis*-$[PtCl_2(NH_3)(2\text{-pic})]$ was reacted with 1.96 mol equiv of $AgNO_3$ (24 h, 323 K), followed by filtration of AgCl, and then addition of 2 mol equiv of 9-EtGH (4–5 d, RT). Recrystallisation from hot water, and slow evaporation yielded **2** as colourless cubes from a solution at pH 3.55.

cis-*[Pt(NH$_3$)(2-pic)(9-EtGH)(9-EtG)]NO$_3$ (**3**)·3.5 H$_2$O*: *cis*-$[PtCl_2(NH_3)(2\text{-pic})]$ was reacted with 1.96 mol equiv of $AgNO_3$ (24 h, 323 K), followed by filtration of AgCl, and then addition of 2 mol equiv of 9-EtGH (24 h, 323 K). Recrystallisation from hot water, and slow evaporation with vapour diffusion of diethyl ether yielded **3** as colourless cubes (at a measured pH of 7.98).

trans-*[Pt(NH$_3$)(2-pic)(9-EtGH)(9-EtG)]NO$_3$ (**4**)·8 H$_2$O*: *trans*-$[PtCl_2(NH_3)(2\text{-pic})]$ was reacted with 1.96 mol equiv of $AgNO_3$ (24 h, RT), followed by filtration of AgCl, and then addition of 2 mol equiv of 9-EtGH (4–5 d, 323 K). Colourless needles of **4** were obtained upon slow evaporation of an aqueous solution at pH 7.83.

NMR spectroscopy: NMR spectra were recorded at 298 K, unless otherwise stated, by using a Bruker DMX500 spectrometer (^{1}H 500.13 MHz), with 5 mm NMR tubes. Spectra were referenced to TSP, via dioxane $\delta = 3.76$ ppm. Water suppression was achieved by presaturation. Spectra were processed by using XWINNMR (Version 3.5, Bruker UK).

Sample preparation: NMR samples were prepared by taking aliquots of the aqueous solutions of the preparations of complexes **1**–**4**. All samples were prepared in H_2O/D_2O 9:1, unless otherwise stated.

pH measurements: The pH values of the solutions were determined by using a Corning 145 pH meter equipped with a micro combination electrode, calibrated with Aldrich buffer solutions at pH 4, 7 and 10. No correction was made for deuterium isotope effects.

pK_a values: These were determined by fitting the NMR pH titration curves (all H_2O/D_2O 9:1) to the Henderson–Hasselbalch equation, assuming fast exchange on the NMR timescale of the protonated and deprotonated forms, by using the program Kaleidagraph (Synergy Software, Reading, PA, USA).

Mass spectrometry: Ion electrospray mass spectrometry was performed by using a Platform II mass spectrometer (Micromass, Manchester, UK). The samples were infused at 8 μL min^{-1} and the ions were produced in an atmospheric pressure ionisation (API)/ESI ion source. The source temperature was 383 K, and the drying gas flow rate was 300 L h^{-1}. A potential of 3.5 kV was applied to the probe tip, and cone voltage gradients of 20–40 V over 200–1000 Da were used. Data acquisition was performed by using a Mass Lynx (V2.5) Windows NT PC data system. All samples were prepared in water.

X-ray crystallography: Diffraction data for all crystals were collected by using $Mo_{K\alpha}$ radiation and a Bruker Smart Apex CCD diffractometer equipped with an Oxford Cryosystems low-temperature device. Data for **2**–**4** were collected at 150 K, but those for **1** were collected at 240 K, as the sample appeared to undergo a phase change between this temperature and 220 K. All structures were solved by using Patterson methods (DIRDIF)[39] and refined by using full-matrix least-squares against F^2 (SHELXTL).[40] Hydrogen atoms were generally placed in calculated positions (see below); only full-weight atoms were refined by using anisotropic displacement parameters. Crystal and refinement data are summarised in Table 1. Additional geometric calculations were accomplished by using the program PLATON,[41] structures were visualised by using SHELXTL-XP[40] and MERCURY.[42]

In structure **1**, the 9-Et groups are disordered. The group attached to N91 is disordered over two positions in the ratio 70:30; the group attached to N92 was modelled similarly; however, the displacement parameters refined to large values, implying that the disorder is more extensive. Similarity restraints were applied to both 9-ethylguanine ligands. The anions and solvent of crystallisation were barely recognisable in difference maps, and were treated by using the method of van der Sluis and Spek,[43] accounting for 150 e per formula unit. The formula, M_r, ρ etc. have all been calculated by assuming that this complex contains $2ClO_4^-$, $2H_2O$ and one acetone molecule per formula unit.

Crystals of **2** were found to be non-merohedrally twinned through a two-fold rotation about [010]. This information was obtained by using the program GEMINI.[44] Diffraction data from both domains were integrated simultaneously (SAINT Version 7),[45] and all data were used for refinement. The twin law can also be expressed by using the following matrix.

$$\begin{pmatrix} -1 & 0 & 0 \\ -0.65 & 1 & -0.33 \\ 0 & 0 & -1 \end{pmatrix}$$

The twinning has an effect on data with $2h+l=3n$; it can be interpreted as a two-fold rotation about the b-axis of a metrically monoclinic supercell with dimensions $a=11.91$, $b=66.75$, $c=12.40$ Å, $\beta=114.3°$, obtained by using the following transformation.[46]

$$\begin{pmatrix} -1 & 0 & 0 \\ 2 & -6 & 1 \\ 0 & 0 & 1 \end{pmatrix}$$

Coset decomposition of $2/m$ with respect to -1 implies that no further twinning needs to be considered.[47]

In **3**, the picoline ligand is disordered by a 180° rotation about the Pt–N bond. The occupancies of the alternative methyl positions were fixed at 0.75 and 0.25 after refinement. The two C–Me bonds were restrained to be of equal length. The molecules of water of crystallisation based on O3W and O4W make unfavourable contacts with the minor disorder component, and the assumption was made that they have the same occupancy as the major component (0.75). The displacement parameter of O3W refined to a large value (0.14 Å^2), and it is possible that in reality its occupancy is less than 0.75; correlation between the occupancy and the displacement parameters means that it is difficult to draw the distinction from X-ray data alone. Hydrogen atoms were located on O1W, O2W and O4W in difference maps; after adjustment of the O–H distances and H-O-H angle to normal values, the entire molecules were treated as freely-rotating rigid groups. Hydrogen atoms were not positioned on O3W.

The complexes in **3** are connected across -1 sites by N41–H41···N41A and N42–H42···N42A (N1–H···N1) hydrogen bonds. Thus, neither H41 nor H42 can be fully occupied, as this would lead to the formation of a very close H···H contact across the inversion centres. Both of these sites were, therefore, assigned occupancies of 0.5, which also ensures charge balance. Similar comments apply to complex **4**.

The solvent and anion regions in the structure of **4** were treated in the same way as in **1**, amounting to 108.5 e per formula unit. The values of M_r, ρ etc. were calculated on the assumption that these regions contain $1NO_3^-$ and $8H_2O$ molecules per formula unit.

CCDC 264834 (**1**), 264835 (**2**), 264836 (**3**) and 264837 (**4**) contain the supplementary crystallographic data for this paper. These data can be obtained free of charge from The Cambridge Crystallographic Data Centre via www.ccdc.cam.ac.uk/data request/cif.

Acknowledgements

We thank AnorMED and AstraZeneca for their support of this work, and the Wellcome Trust for provision of NMR facilities in the Edinburgh Protein Interaction Centre (EPIC). We are grateful to Professor Giovanni Natile and colleagues in the EC COST Action D20 for stimulating discussions.

[1] E. R. Jamieson, S. J. Lippard, *Chem. Rev.* **1999**, *99*, 2467–2498.
[2] A. M. J. Fichtinger-Schepman, J. L. van der Veer, J. H. J. den Hartog, P. H. M. Lohman, J. Reedijk, *Biochemistry* **1985**, *24*, 707–713.
[3] S. O. Ano, F. P. Intini, G. Natile, L. G. Marzilli, *J. Am. Chem. Soc.* **1997**, *119*, 8570–8571.
[4] J. S. Saad, T. Scarcia, K. Shinozuka, G. Natile, L. G. Marzilli, *Inorg. Chem.* **2002**, *41*, 546–557.
[5] J. Holford, F. Raynaud, B. A. Murrer, K. Grimaldi, J. A. Hartley, M. Abrams, L. R. Kelland, *Anti-Cancer Drug Des.* **1998**, *13*, 1–18.
[6] Y. Chen, Z. Guo, S. Parsons, P. J. Sadler, *Chem. Eur. J.* **1998**, *4*, 672–676.
[7] K. Harrap, *The Institute of Cancer Research Study Report*, November **1992**, unpublished results, AnorMED Inc.
[8] B. Lippert, G. Raudaschl, C. J. L. Lock, P. Pilon, *Inorg. Chim. Acta* **1984**, *93*, 43–50.
[9] H. Schöllhorn, G. Raudaschl-Sieber, G. Müller, U. Thewalt, B. Lippert, *J. Am. Chem. Soc.* **1985**, *107*, 5932–5937.
[10] S. E. Sherman, D. Gibson, A. H.-J. Wang, S. J. Lippard, *J. Am. Chem. Soc.* **1988**, *110*, 7368–7381.
[11] G. Frommer, H. Schöllhorn, U. Thewalt, B. Lippert, *Inorg. Chem.* **1990**, *29*, 1417–1422.
[12] G. Schröder, J. Kozelka, M. Sabat, M.-H. Fouchet, R. Beyerle-Pfnür, B. Lippert, *Inorg. Chem.* **1996**, *35*, 1647–1652.
[13] R. E. Cramer, P. L. Dahlstrom, M. J. T. Seu, T. Norton, M. Kashiwagi, *Inorg. Chem.* **1980**, *19*, 148–154.
[14] R. W. Gellert, R. Bau, *J. Am. Chem. Soc.* **1975**, *97*, 7379–7380.
[15] S. Grabner, J. Plavec, N. Bukovec, D. Di Leo, R. Cini, G. Natile, *J. Chem. Soc. Dalton Trans.* **1998**, 1447–1451.
[16] R. Cini, S. Grabner, N. Bukovec, L. Cerasino, G. Natile, *Eur. J. Inorg. Chem.* **2000**, 1601–1607.
[17] R. K. O. Sigel, E. Freisinger, B. Lippert, *J. Biol. Inorg. Chem.* **2000**, *5*, 287–299.
[18] F. Schwarz, B. Lippert, H. Schöllhorn, U. Thewalt, *Inorg. Chim. Acta* **1990**, *176*, 113–121.
[19] R. Beyerle-Pfnür, B. Brown, R. Faggiani, B. Lippert, C. J. L. Lock, *Inorg. Chem.* **1985**, *24*, 4001–4009.
[20] G. Schröder, B. Lippert, M. Sabat, C. J. L. Lock, R. Faggiani, B. Song, H. Sigel, *J. Chem. Soc. Dalton Trans.* **1995**, 3767–3775.

[21] R. Faggiani, B. Lippert, C. J. L. Lock, R. A. Speranzini, *Inorg. Chem.* **1982**, *21*, 3216–3225.
[22] G. Schröder, M. Sabat, I. Baxter, J. Kozelka, B. Lippert, *Inorg. Chem.* **1997**, *36*, 490–493.
[23] B. Lippert, *J. Am. Chem. Soc.* **1981**, *103*, 5691–5697.
[24] B. Lippert, *Met. Ions Biol. Syst.* **1996**, *33*, 106–141.
[25] S. Yao, J. P. Plastaras, L. G. Marzilli, *Inorg. Chem.* **1994**, *33*, 6061–6077.
[26] C. Meiser, E. Freisinger, B. Lippert, *J. Chem. Soc. Dalton Trans.* **1998**, 2059–2064.
[27] A. Schreiber, M. S. Lüth, A. Erxleben, E. C. Fusch, B. Lippert, *J. Am. Chem. Soc.* **1996**, *118*, 4124–4132.
[28] O. Krizanovic, M. Sabat, R. Beyerle-Pfnür, B. Lippert, *J. Am. Chem. Soc.* **1993**, *115*, 5538–5548.
[29] I. Dieter-Wurm, M. Sabat, B. Lippert, *J. Am. Chem. Soc.* **1992**, *114*, 357–359.
[30] E. Freisinger, I. B. Rother, M. S. Lüth, B. Lippert, *Proc. Natl. Acad. Sci. USA* **2003**, *100*, 3748–3753.
[31] R. K. O. Sigel, S. M. Thompson, E. Freisenger, F. Glahé, B. Lippert, *Chem. Eur. J.* **2001**, *7*, 1968–1980.
[32] E. Freisenger, S. Meier, B. Lippert, *J. Chem. Soc. Dalton Trans.* **2000**, 3274–3280.
[33] H. C. Wong, K. Shinozuka, G. Natile, L. G. Marzilli, *Inorg. Chim. Acta* **2000**, *297*, 36–46.
[34] N. Margiotta, P. Papadia, F. P. Fanizzi, G. Natile, *Eur. J. Inorg. Chem.* **2003**, *6*, 1136–1144.
[35] A. T. M. Marcelis, J. L. van der Veer, J. C. M. Zwetsloot, J. Reedijk, *Inorg. Chim. Acta* **1983**, *78*, 195–203.
[36] R. Griesser, G. Kampf, L. E. Kapinos, S. Komeda, B. Lippert, J. Reedijk, H. Sigel, *Inorg. Chem.* **2003**, *42*, 32–41.
[37] B. Song, J. Zhao, R. Griesser, C. Meiser, H. Sigel, B. Lippert, *Chem. Eur. J.* **1999**, *5*, 2374–2387.
[38] G. B. Kauffman, D. O. Cowan, *Inorg. Synth.* **1963**, *7*, 239–245.
[39] P. T. Beurskens, G. Beurskens, W. P. Bosman, R. de Gelder, S. Garcia-Granda, R. O. Gould, R. Israel, J. M. M. Smits, The DIRDIF96 Program System, Technical Report of the Crystallography Laboratory, University of Nijmegen, Nijmegen (The Netherlands), **1996**.
[40] G. M. Sheldrick, SHELXTL, University of Göttingen, Göttingen (Germany), **2001**.
[41] A. L. Spek, PLATON, A Multipurpose Crystallographic Tool, Utrecht University, Utrecht (The Netherlands), **2004**.
[42] I. J. Bruno, J. C. Cole, P. R. Edgington, M. Kessler, C. F. Macrae, P. McCabe, J. Pearson, R. Taylor, *Acta Crystallogr. Sect. B* **2002**, *58*, 389–397.
[43] P. van der Sluis, A. L. Spek, *Acta Crystallogr. Sect. A* **1990**, *46*, 194–201.
[44] R. A. Sparks, GEMINI, Bruker AXS, Madison, Wisconsin (USA), **1999**.
[45] Bruker AXS, SAINT Version 7, Madison, Wisconsin (USA), 2003.
[46] Y. Le Page, *J. Appl. Crystallogr.* **1982**, *15*, 255–259.
[47] H. D. Flack, *Acta Crystallogr. Sect. A* **1987**, *A43*, 564–568.

Received: February 3, 2005
Published online: May 6, 2005